ORIGINAL ARTICLE

Hatem Alkadhi · Bernhard Baumert ·
Simon Wildermuth · Konrad E. Bloch ·
Borut Marincek · Thomas Boehm

Coronal thick CT reconstruction: an alternative for initial chest radiography in trauma patients

Abstract It has been proposed that the imaging workup of trauma patients be accelerated by omitting the initial chest radiography (CR) and directly performing a computed tomography (CT); however, the baseline CR is then lacking. The purpose of this study was to assess if coronal thick reconstructions generated from chest CT could present an adequate alternative for CR. Sixty trauma patients underwent bedside CR and multidetector row chest CT in the emergency room. The image quality of thoracic anatomical structures, the diagnostic accuracy for chest pathology, and the depiction of indwelling devices were assessed on both modalities. Main pulmonary arteries and perihilar bronchi were equally visualized with both modalities. Central bronchi, retrocardial lung parenchyma, diaphragm, descending aorta, and vertebral pedicles were better visualized on thick CT reconstructions, whereas peripheral lung vessels were better depicted on CR ($p<0.05$). The accuracy to delineate various pathological findings did not differ between both modalities, except for a higher sensitivity to diagnose bronchial cuffing on CR ($p<0.05$). The location of indwelling devices was similarly and correctly depicted with both modalities. Coronal thick CT reconstructions provide a similar image quality and diagnostic accuracy compared with CR. These reconstructions may serve as an equivalent baseline image in trauma patients in whom emergency radiological evaluation has to be accelerated.

Keywords Emergency · Chest radiography · Computed tomography · Coronal thick reconstruction

H. Alkadhi · B. Baumert · S. Wildermuth ·
B. Marincek · T. Boehm
Institute of Diagnostic Radiology,
University Hospital Zurich,
Zurich, Switzerland

K. E. Bloch
Pulmonary Division, Department of Internal Medicine,
University Hospital Zurich,
Zurich, Switzerland

T. Boehm (✉)
Department of Radiology, Spitäler Chur AG,
Loestrasse 170,
CH-7000 Chur, Switzerland
e-mail: Thomas_Boehm@gmx.net
Tel.: +41-81-2566452
Fax: +41-81-2566685

Introduction

The emergency management of a trauma patient relies on the concept of the advanced trauma life support (ATLS), which has been developed in response to the need for a safe, consistent, standardized, and effective way to initially evaluate and resuscitate patients with multiple injuries [1–3]. The term "golden hour" characterizes the fact that the morbidity and mortality of trauma patients are affected if care is not instituted within the first hour after injury. To comply with this concept, radiological examinations must be fast, systematic, and as complete as possible.

In patients with acute chest trauma, bedside chest radiography (CR) is the most common initial imaging workup method in the emergency room [4]. CR is used to screen for the presence of life-threatening conditions that necessitate immediate intervention, to evaluate injuries that require intervention without further diagnostic workup, to assess abnormalities that require further investigation, or to document the positioning of indwelling devices. Especially if the presumed injury did not severely affect the chest, a CR might suffice, obviating the need for a chest computed tomography (CT). Hence, chest CT is indicated only in a subset of patients depending on the severity and site of injury and on the hemodynamic stability of the patient. Chest CT should be also performed when the image quality of bedside CR is low, having limited diagnostic accuracy, which is often the case in the emergency setting [5–7]. Since time is crucial in the emergency workup of the trauma patient, it would be desirable to gain all necessary information by a single imaging method. Therefore, omitting CR in patients who anyway undergo CT of the chest as part of their imaging evaluation was suggested by

4

several authors [8–10]. This would also result in a reduction of patient discomfort, costs, and irradiation [11]. On the other hand, the initial CR serves as an important baseline examination for further treatment monitoring and is considered a necessary tool by most clinicians. Therefore, it is still performed as a part of the initial workup in most trauma centers.

New-generation multidetector row CT (MDCT) scanners acquire high-resolution data with nearly isotropic voxels, allowing multiplanar reconstructions (MPR) of the CT data in any arbitrary plane. When performing coronal thick MPR from MDCT data of the chest, images can be obtained, which qualitatively resemble a conventional bedside CR. When it has been decided that the imaging evaluation of trauma patients be accelerated by immediately performing a CT (and to omit the CR), such coronal thick MPR could serve as an alternative equivalent for the initial bedside CR. Time could be saved in the first critical hour of emergency management, without lacking a baseline examination for further treatment monitoring and follow-up. We therefore assessed the image quality and diagnostic accuracy of coronal thick MPR reconstructed from MDCT data and compared them with the initial bedside CR of trauma patients in the emergency room.

Materials and methods

From June to October 2003, 60 trauma patients (26 women, 34 men; age range 17–67 years, mean age 48 years) were referred to our emergency department, a level I European trauma center, for an MDCT of the chest. Causes of injuries were traffic accidents (n=29), falls (n=17), and domestic (n=9) and occupational accidents (n=5). All patients initially received a bedside CR and, afterwards, a chest MDCT within the first hour of their stay in the emergency room. The patients had the following extrathoracic injuries: head injuries in 46%; renal, splenic, and liver injuries in 27%; sacral, lumbar, or cervical spine fractures in 71%; and upper or lower extremity fractures in 78% of the patients. Fifty-six patients (93%) underwent, in addition, an abdomino–pelvic CT, and 51 patients (85%), an additional head CT. The radiological workup in all patients was not performed for study purposes but for clinical indications. The study protocol was approved by the local ethics committee.

Chest radiography

The bedside CR was obtained in the supine position with a focus-film distance of 100 cm using a ceiling-mounted x-ray setup in the emergency room (Siemens Mobilett XT, Siemens, Erlangen, Germany). A fixed tube voltage of 75 kV and a tube current of 3.0 to 3.6 mA were manually adjusted by the x-ray technician according to the patient's size. No automatic exposure control and no antiscatter grids were employed. When possible, the bedside CR was taken in inspiration. Image acquisition was performed with

a storage phosphor plate system (ADC Compact with ADC MD40 phosphor plates, Agfa-Gevaert, Mortsel, Belgium). For image postprocessing, the routine parameters defined at our institution for bedside CR were used.

Multidetector row CT

CT scans were performed on a 16-channel MDCT scanner (Sensation 16, Siemens Medical Solutions, Forchheim, Germany), which is situated in the emergency room. If possible, CT was acquired with inspiratory breath-hold and with elevated arms. For the whole body examination, 150 ml nonionic, iodinated, low-osmolar contrast agent (Visipaque 270, Amersham Health, Buckinghamshire, UK) was injected into a cubital vein at a flow rate of 3 ml/s and subsequently flushed by 30 ml saline fluid using a power injector (Envision CT, Medrad Inc., Indianola, PA, USA). The imaging volume extended from the apices of the lungs to the diaphragm. The scanning parameters were the following: collimation, 16×1.5 mm; table feed, 24 mm/rotation; increment, 1 mm; tube potential, 140 kV; tube current, 140 mA. Two sets of axial images were reconstructed: The first set, with a slice width of 5 mm and a reconstruction interval of 4 mm, was used for filming and hospital-wide electronic image distribution, and the second set, with a slice width of 2 mm and a reconstruction increment of 1 mm, was used for image reading and postprocessing. Both sets of axial images were reconstructed twice using a medium soft kernel (BF30) for soft tissue imaging and a high-resolution kernel (BF60) for lung imaging. Coronal thick MPR of the chest (MPR thickness, 500 mm) was reconstructed from the 2 mm/1 mm BF60 axial datasets in the coronal plane using the standard 3D postprocessing software of the secondary CT console (Sensation Wizard, software version VA70, Siemens Medical Solutions). The large standardized MPR thickness of 500 mm was used to take into account differences in patient size and morphology and to avoid losing time for individual patient adjustment. The CT table, which would otherwise interfere with the patients' structures, was removed from the dataset using the standard 3D image editing tools. Window settings for MPR were adjusted manually by two radiologists in consensus to obtain an image appearance that is similar to a correctly exposed bedside CR.

Both CR and coronal thick MPR were printed out on hard copy films (size, 14×11 cm) using a laser imaging system (Drystar 5500, Agfa-Gevaert).

Image reading

Image readout was performed in two steps. First, image reading was performed by one experienced radiologist using the axial CT images and all other available images, including follow-up evaluations and all clinical data. The results of this reading were used as gold standard for the assessment of diagnostic accuracy with CR and thick MPR. This assessment was limited to a

binary scale (i.e., pathological changes of a certain anatomical structure present or not). In a second step, 10 weeks after the first reading, the hardcopies of the CR and thick MPR were presented in a random order to two independently working chest radiologist. They were blinded to the clinical data, the results of the gold standard reading, and to the results of the other viewing modality. The reviewers were asked to rate each image on a defined Likert scale with respect to the exposure quality, windowing, artifacts, visibility of critical anatomic structures, pathological findings, and indwelling devices. More specifically, the following scores were applied: exposure quality of CR: 1=normal exposure; 2=underexposure; 3=overexposure. Stair step artifacts of the bronchi on thick MPR were scored as the following: 1=no stair step artifacts; 2=stair step artifacts less than 1 mm; 3=stair step artifacts more than 1 mm; 4=severe distortion of the bronchial wall due to stair step artifacts.

The anatomical landmarks, including central and perihilar bronchi, lung vessels in the lung periphery, central pulmonary arteries, retrocardial lung parenchyma, diaphragm, descending aorta, and pedicles of the thoracic spine, were rated on both modalities with the following scores: 1=excellent visibility; 2=good visibility; 3=fair visibility; 4=bad visibility; 5=anatomical structure not visible.

The pathological findings, including pneumothorax, bronchial cuffing, perihilar congestion, atelectasis, consolidation/lung contusion, pleural effusion/hemothorax, pleural capping, soft tissue emphysema, fractures of the ribs and shoulder girdle, mediastinal widening, pericardial effusion, pneumomediastinum/pneumopericardium, and vertebral fractures, were assessed on both modalities using the following scores: 1=definitely present; 2=probably present;

3=indefinite; 4=probably not present; 5=definitely not present.

The indwelling devices, including endotracheal tube, central venous catheter, and pleural drainage tube, were evaluated on both modalities using the following scores: 1=definitely correct location; 2=probably correct location; 3=indefinite, assessment not possible; 4=probably incorrect location; 5=definitely incorrect location.

Statistical analysis

Statistical analysis was performed using a commercially available software (SSPS 11.5 for Windows, SPSS Inc., Chicago, IL, USA). Interobserver agreement between both readers was calculated by using κ statistics. According to Landis and Koch [12], a κ value of 0 indicated poor agreement; a κ value of 0.01–0.20, slight agreement; a κ value of 0.21–0.40, fair agreement; a κ value of 0.41–0.60, moderate agreement; a κ value of 0.61–0.80, good agreement; and a κ value of 0.81–1.00, excellent agreement. Subjective certainty was calculated by reclassifying the initial scores: former scores 1 and 5 (definitely present/ definitely not present) were pooled to score 1 (high diagnostic certainty), and scores 2 and 4 (most probably present/most probably not present) were pooled to score 2 (medium diagnostic certainty); score 3 (assessment not possible) remained score 3 (low diagnostic certainty). Comparisons of these scores from both viewing modalities were made using the Wilcoxon signed-rank test. For the evaluation of the diagnostic accuracy of pathological findings and location of indwelling devices, scores 1 and 2 (definitely and probably present/correct location) were categorized as pathologic/correct location, and scores 4 and

Table 1 Mean scores±standard deviations and interobserver agreement for image quality of anatomical landmarks

Anatomical landmarks	CR	MPR	p Value	CR κ	MPR κ
MPR better					
Retrocardial lung parenchyma	2.94±0.96	1.72±0.87	0.015	0.845	0.951
Right diaphragm	2.75±0.99	1.95±0.97	0.048	0.799	0.837
Left diaphragm	3.16±0.73	2.13±0.89	0.015	0.811	0.858
Descending aorta	3.47±0.96	2.51±0.97	0.006	0.848	0.936
Pedicles of the thoracic spine	3.75±1.04	2.24±0.58	0.013	0.749	0.819
Right main bronchus	3.35±0.72	2.08±0.58	0.012	0.798	0.858
Left main bronchus	3.51±0.78	2.27±0.66	0.016	0.844	0.901
CR better					
Peripheral lung vessels—upper right	1.79±0.63	2.69±0.54	0.016	0.914	0.851
Peripheral lung vessels—lower right	1.94±0.51	2.42±0.46	0.049	0.897	0.879
Peripheral lung vessels—upper left	1.89±0.48	2.33±0.53	0.018	0.921	0.743
Peripheral lung vessels—lower left	1.72±0.42	2.24±0.56	0.016	0.933	0.833
CR and MPR equal					
Right main pulmonary artery	2.85±0.79	3.27±0.62	0.564	0.791	0.898
Left main pulmonary artery	2.66±0.58	3.19±0.45	0.317	0.806	0.829
Right perihilar bronchi	3.14±0.84	2.24±0.61	0.705	0.879	0.917
Left perihilar bronchi	3.25±0.59	2.31±0.73	0.092	0.835	0.897

CR Chest radiograph, *MPR* multiplanar reconstruction, *CR* κ and *MPR* κ interobserver agreement

5 (probably and definitely not present/incorrect) were categorized as not pathologic/incorrect location. Sensitivity, specificity, accuracy, positive predictive values (PPV), and negative predictive values (NPV) were then calculated with the results from axial CT image reading and all other available images, including follow-up evaluations and all clinical data as gold standard. Differences between MPR and portable chest film were computed from chi-square tests of contingency. Statistically significant differences were indicated by p values of less than 0.05.

Results

All 60 CR and MDCT examinations were performed without any technical complications. The mean time interval from the completion of the CR through the completion of the MDCT scan was 28 ± 10 min ($\pm$standard deviation). The reconstruction of thick MPR required an average time of 31 s (range 19–41 s).
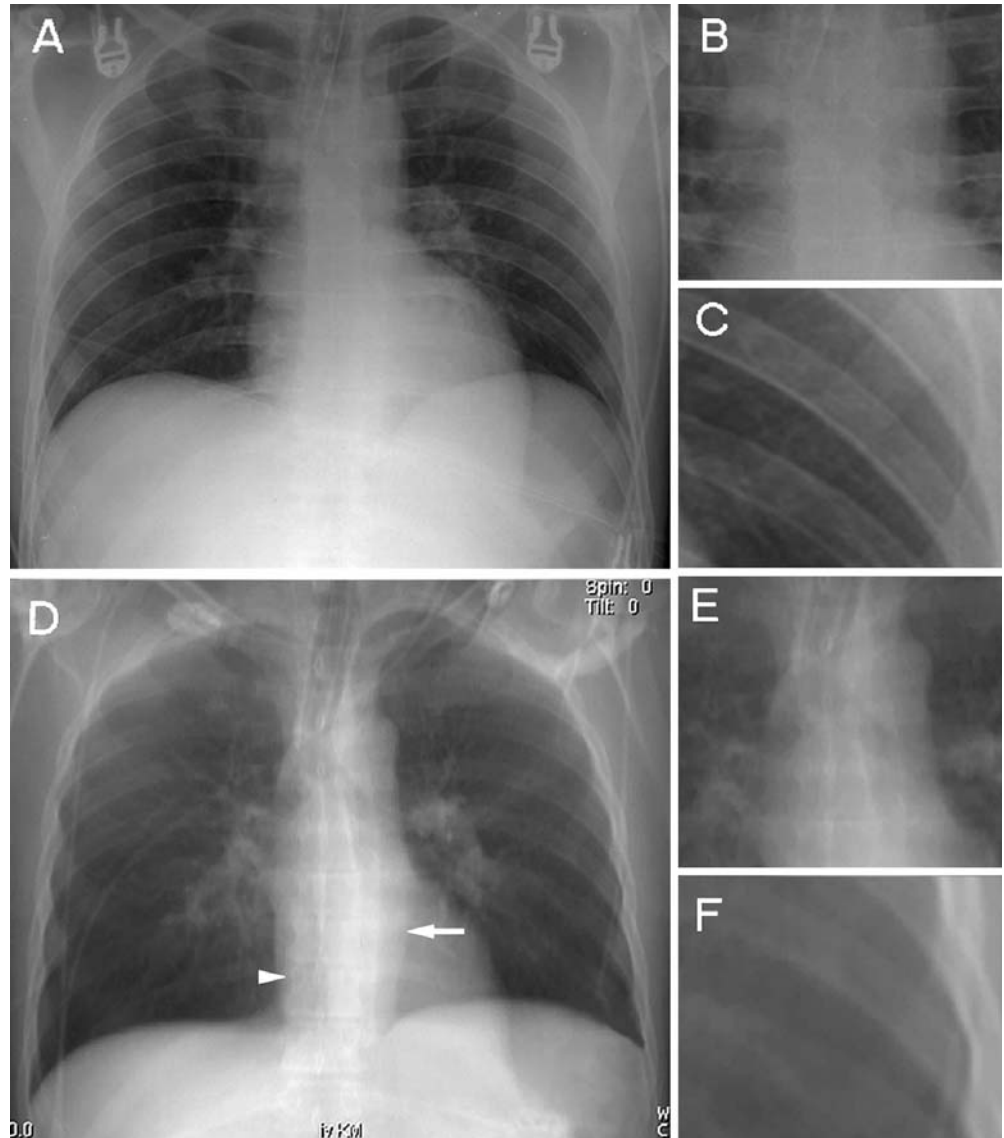
Image quality

The exposure quality of CR was rated as normal in 44 patients (73%) by reader 1 and in 46 (77%) by reader 2, as underexposed in 12 patients (20%) by reader 1 and in 11 patients (18%) by reader 2, and as overexposed in 4 patients (7%) by reader 1 and in 3 patients (5%) by reader 2. Thick MPR showed, on average, stair step artifacts of the both main bronchi less than 1 mm (mean score$_{MPR,\ both\ readers,\ right}$=$1.53 \pm 0.47$, mean score$_{MPR,\ both\ readers,\ left}$=$1.58 \pm 0.27$).

Anatomical landmarks

Table 1 summarizes the results for visualization of critical anatomical landmarks using CR and thick MPR. The ratings did not differ significantly between the two readers for all anatomical structures ($p > 0.05$). The interobserver agreement ranged from good to excellent. The rating

Fig. 1 A 47-year-old male patient after motorcycle accident. There was no pathological finding demonstrating a similar image quality, with only slight differences between chest radiography (CR; **a**–**c**) and coronal thick multiplanar reconstruction (MPR; **d**–**f**). The trachea and both main bronchi were better visualized on thick MPR when compared with CR (**b** and **e**, *enlarged images*), whereas peripheral pulmonary vessels are better depicted on CR (**c** and **f**, *enlarged images*). Retrocardial lung parenchyma, descending aorta (*arrow*), and pedicles of the thoracic spine (*arrowhead*) are superiorly visualized on thick MPR (**d**). The location of the endotracheal tube can be sufficiently assessed with both modalities (**b** and **e**, *enlarged images*)

Table 2 Sensitivity, specificity, accuracy, positive predictive value (PPV), negative predictive value (NPV), and interobserver agreement of pathologic findings and location of indwelling devices

Pathology/Indwelling devices	N	Sensitivity		Specificity		Accuracy		PPV		NPV		κ	
		CR	MPR	CR	MPR	CR	MPR	CR	MPR	CR	MPR	CR	MPR
Equal accuracy													
Pneumothorax	17	60	53	100	97	90	89	100	88	91	86	0.943	0.884
Perihilar congestion	31	68	77	82	76	75	77	80	78	71	75	0.843	0.882
Atelectasis	22	84	90	97	100	90	96	94	100	93	95	0.931	0.820
Consolidation/Contusion	17	81	68	100	97	73	68	81	74	91	85	0.916	0.914
Pleural effusion /hemothorax	15	70	93	87	97	74	80	81	93	85	97	0.753	0.863
Chest wall emphysema	12	97	78	95	96	88	93	77	90	90	93	0.775	0.845
Rib fracture	11	80	90	88	91	86	92	80	71	94	97	0.915	0.832
Shoulder girdle fracture	8	63	57	94	92	92	88	63	50	96	94	0.876	0.771
Thoracic spine fracture	4	75	25	97	98	98	93	100	50	98	95	0.913	0.719
Mediastinal widening	6	63	75	94	96	91	93	71	75	94	96	0.901	0.965
Pneumomediastinum	8	50	63	100	96	88	91	57	71	92	94	0.902	0.813
Pericardial effusion	3	66	33	96	96	95	93	50	33	98	96	0.855	0.797
Endotracheal tube	42	98	95	100	100	98	97	100	100	86	93	0.972	0.954
Central venous catheter	19	95	94	100	100	97	98	100	100	96	98	0.920	0.989
Pleural drainage tube	11	100	100	100	100	100	100	100	100	100	100	0.925	0.971
CR more accurate													
Bronchial cuffing	29	86	71	93	87	90	78	92	83	87	75	0.867	0.817

CR Chest radiograph, *MPR* multiplanar reconstruction, *N* number of pathologic findings, κ interobserver agreement

results were therefore grouped together, and the mean scores±standard deviations of both readers were calculated. Thick MPR performed better in visualizing both main bronchi, diaphragm, retrocardial lung parenchyma, descending aorta, and thoracic spine pedicles. CR visualized peripheral lung vessels in all four quadrants with a higher quality than thick MPR. The visualization of perihilar bronchi and central pulmonary arteries did not differ between the two techniques. An example for the visual-ization of chest anatomy with CR and thick MPR is demonstrated in Fig. 1.

Pathology

Table 2 lists the sensitivity, specificity, accuracy, PPV, and NPV for the detection of pathological findings and for the localization of indwelling devices with CR and thick MPR.

Table 3 Diagnostic certainty for the assessment of pathology and location of indwelling devices for both readers

Pathologic findings/indwelling devices	Diagnostic certainty		
	CR	MPR	*p* Value
MPR better			
Atelectasis	1.56±0.68	1.22±0.59	0.022
Pleural effusion/Hemothorax	1.60±0.66	1.25±0.39	0.026
Chest wall emphysema	1.49±0.47	1.19±0.39	0.038
Mediastinal widening	1.49±0.51	1.30±0.42	0.049
Pneumomediastinum	1.63±0.67	1.43±0.60	0.042
CR better			
Pneumothorax	1.54±0.34	2.13±0.45	0.012
Bronchial cuffing	1.29±0.49	1.94±0.83	0.008
Consolidation/Contusion	1.43±0.56	2.08±0.71	0.008
Shoulder girdle fracture	1.20±0.59	1.79±0.55	0.009
Thoracic spine fracture	1.29±0.32	1.63±0.53	0.024
CR and MPR equal			
Perihilar congestion	1.71±0.52	1.54±0.34	0.052
Rib fracture	1.31±0.27	1.45±0.73	0.081
Pericardial effusion	1.32±0.49	1.23±0.42	0.171
Endotracheal tube	1.24±0.38	1.40±0.38	0.259
Central venous catheter	1.29±0.25	1.39±0.30	0.452
Pleural drainage tube	1.31±0.27	1.38±0.44	0.231

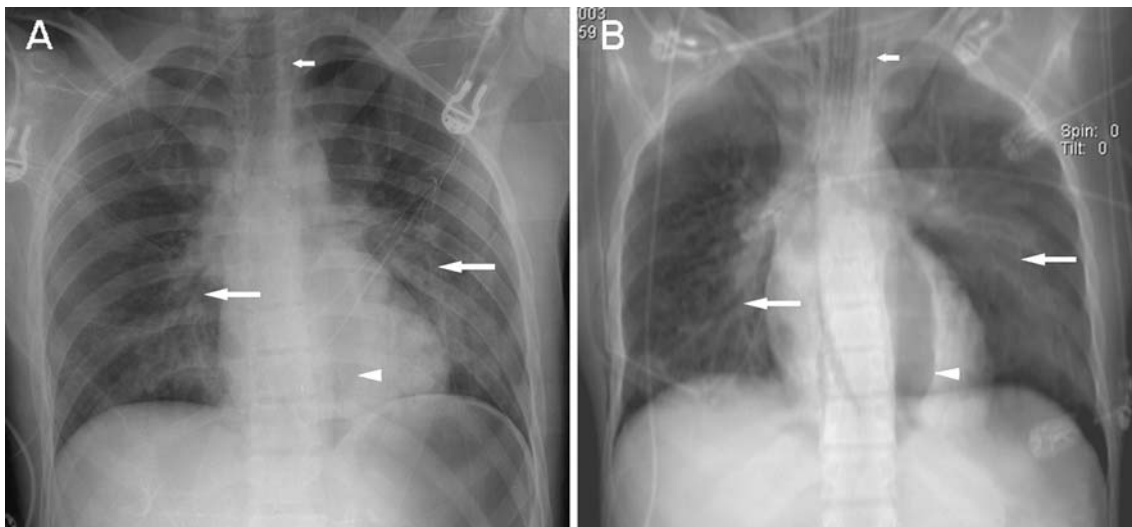*CR* Chest radiograph, *MPR* multiplanar reconstruction

Fig. 2 CR (**a**) and coronal thick MPR (**b**) images demonstrating different traumatic chest injuries of a 20-year-old male patient after a 15-m downfall. Lung contusions (*large arrows*) and mediastinal emphysema (*small arrows*) were similarly visualized on both CR and thick MPR. The ventral pneumothorax on the *left* side (*arrowheads*) is better depicted on thick MPR and was initially missed on CR by both readers, possibly because of an increase in the time interval between CR and computed tomography (CT). The pleural drainage on the *right* and the endotracheal tube were introduced before CT

Statistically significant differences were only present for the sensitivity for the detection of bronchial cuffing, with a better performance of CR compared with MPR. The interobserver agreement for the assessment of pathology ranged from good to excellent for both imaging modalities (see Table 2).

Table 3 lists the diagnostic certainty and corresponding *p* values of both methods for all pathological findings and for the localization of indwelling devices. The diagnostic certainty was higher for thick MPR for the diagnosis of atelectasis, pleural effusion/hemothorax, chest wall emphysema, mediastinal widening, and mediastinal emphysema. Diagnostic certainty was higher for CR for diagnosing pneumothorax, bronchial cuffing, consolidation/contusion, and fractures of the shoulder girdle and spine. The readers were equally certain with both methods in diagnosing perihilar congestion, pericardial effusion, and rib fractures (see Table 3).

Figure 2 demonstrates the visualization of some pathological findings with CR and thick MPR.

Indwelling devices

Both CR and thick MPR similarly and correctly visualized the position of the endotracheal tube, central venous catheter, and pleural drainage tube. The accuracy and diagnostic certainty did not differ, and the interobserver agreement was excellent for both imaging modalities (see Tables 2 and 3).

Discussion

The radiological workup of trauma patients has to be accomplished timely, efficiently, and accurately. It has been therefore proposed that imaging in the emergency setting should be limited to a single CT examination, thereby saving important time [8–10]. This study demonstrates that coronal thick MPR generated from MDCT data depicts anatomy and pathology and documents the location of indwelling devices with a similar quality when compared with conventional bedside CR. Consequently, in trauma patients in whom the initial CR is omitted and who directly undergo MDCT, an adequate equivalent to the omitted CR can be reconstructed for subsequent treatment monitoring on the intensive care unit or ward.

CT is nowadays a widely used and versatile imaging modality for emergency patient management [8–10, 13–15]. Major recent developments have led to the introduction of MDCT in the emergency setting, with fast data acquisition and tailored MDCT protocols, allowing even severely injured and hemodynamically unstable patients to have a CT [13, 14]. Besides the high sensitivity for the detection of various traumatic chest injuries [16], MDCT enables one to scan, with a sub-millimeter resolution, large areas of the body during a single breath-hold. This high *z*-plane resolution results in nearly isotropic voxels (i.e., voxels with almost the same dimensions in the *x*, *y*, and *z* axes), which allow one to perform high-quality 2D and 3D reconstructions in any plane and desired thickness.

In this study, the accuracy of coronal thick MPR in identifying thoracic anatomy, pathology, and indwelling devices was comparable with that of CR. However, some differences in image quality and diagnostic accuracy between modalities were noted, which may be explained on methodological grounds.

Respiratory motion artifacts may decrease the image quality of axial MDCT images and, consequently, also the reconstructed thick MPR. They affect the image quality of CR in a much lesser degree because of the shorter acquisition time (10 ms for CR vs approximately 9 s for MDCT). If possible, the patient is asked to hold his breath

during the CT scan, or if mechanically ventilated, the ventilation is stopped during the scan. However, in the emergency setting, the patient's compliance to hold breath is often limited, and the marginal respiratory and cardiovascular function may not allow a pause in ventilation.

The currently used axial CT resolution (2 mm slice width) leads to an impaired visualization of small pulmonary structures such as peripheral lung vessels and may result in stair step artifacts of the central bronchi. Increasing the axial resolution, however, is currently not feasible in the emergency setting due to more time-consuming reconstructions and because of the longer image loading and viewing times of larger CT datasets.

On the other hand, some anatomical structures were better visualized on thick MPR than on CR. This may be explained by the comparably higher radiation dose applied during CT (approximately 3 mSv for MDCT vs 0.1 mSv for CR), resulting in a better definition of structures that are located behind each other, such as the retrocardial lung parenchyma, both main bronchi, and the pedicles of the thoracic spine.

In addition, geometric distortion in conventional imaging, which is due to an unequal magnification of different structures, may also contribute to a reduction of image quality in CR. This distortion is a well-known and accepted limitation for accurate measurements of thoracic organs, a phenomenon that does not occur in reconstructed images based on volumetric CT datasets.

A more simple explanation can be given for the better visualization of the descending aorta on thick MPR, which is most likely due to the intravenous contrast material administered for CT.

Finally, differences between both modalities concerning pathological findings may also be the result of the time delay between the two examinations. Although keeping this delay as short as possible (less than 1 h), various drugs supporting the patient's cardiovascular function or indwelling devices, such as chest tubes, may interfere with the imaging appearance on the corresponding modality. For example, bronchial cuffing often caused by edema may rapidly improve when the patient is stabilized before undergoing CT. Similarly, fractures could be dislocated or readjusted during the patient's transport from the emergency table to the CT scanner, and also, a pneumothorax may change during this time interval.

Concerning the relatively low accuracy of thick MPR for the detection of certain pathological findings, it is necessary to bear in mind that the most accurate diagnostic information is obtained anyway from axial CT images. Since the idea of this study is the replacement, in the future, of the initial bedside CR by thick MPR, the most important statistical comparison is that of the diagnostic accuracy between modalities, which, in fact, showed a high concordance.

This study does not advocate to omit CR in the emergency setting but to provide an alternative image resembling CR when performing chest CT anyway. Therefore, the unquestionable higher radiation dose of CT when compared with CR is not an argument against the suggested thick MPR method. In contrast, when replacing the initial CR by thick MPR, the totally applied radiation dose to the individual patient is even slightly reduced.

We have to acknowledge the following limitations. Despite the relatively large patient number, the incidence of certain pathological findings (such as fractures or mediastinal pathology) is relatively low. This may limit the calculated descriptive statistics regarding sensitivity, specificity, PPV, NPV, and diagnostic accuracy. On the other hand, this does not apply for the assessment of other pathological findings and for anatomical structures that were assessed for the entire patient population in a high number. We did not assess the value of CT scanograms as an alternative method for CR instead of thick MPR. The scanograms obtained in this study were acquired in a single frontal view and with a low radiation dose, and although not performing a direct quantitative comparison, we considered their image quality as being insufficient to be a reliable alternative for CR.

In conclusion, coronal thick MPR generated from MDCT data provide chest images with a quality and diagnostic accuracy comparable with the bedside CR in trauma patients. They may be used as an equivalent baseline image for subsequent follow-up in trauma patients, in whom the initial CR is omitted to accelerate the diagnostic workup. Further prospective outcome studies have to assess the practical usefulness of thick MPR when replacing the initial CR in the clinical setting.

References

1. Bell RM, Krantz BE, Weigelt JA (1999) ATLS: a foundation for trauma training. Ann Emerg Med 34:233–237
2. Olson CJ, Arthur M, Mullins RJ, Rowland D, Hedges JR, Mann NC (2001) Influence of trauma system implementation on process of care delivered to seriously injured patients in rural trauma centers. Surgery 130:273–279
3. American College of Surgeons Committee on Trauma (1997) Student course manual. Advanced trauma life support for doctors. American College of Surgeons, Chicago
4. Schweiberer L, Nast-Kolb D, Duswald KH, Waydhas C, Muller K (1987) Polytrauma-treatment by the staged diagnostic and therapeutic plan. Unfallchirurg 90:529–538
5. Massarutti D, Berlot G, Saltarini M, Trillo G, D'Orlando L, Pessina F, Modesto A, Meduri S, Da Ronch T, Carchietti E (2004) Abdominal ultrasonography and chest radiography are of limited value in the emergency room diagnostic work-up of severe trauma patients with hypotension on the scene of accident. Radiol Med (Torino) 108:218–224
6. Collins JA, Samra GS (1998) Failure of chest X-rays to diagnose pneumothoraces after blunt trauma. Anaesthesia 53:74–78
7. Neff MA, Monk JS Jr., Peters K, Nikhilesh A (2000) Detection of occult pneumothoraces on abdominal computed tomographic scans in trauma patients. J Trauma 49:281–285
8. Leidner B, Adiels M, Aspelin P, Gullstrand P, Wallen S (1998) Standardized CT examination of the multitraumatized patient. Eur Radiol 8:1630–1638

9. Low R, Duber C, Schweden F, Lehmann L, Blum J, Thelen M (1997) Whole body spiral CT in primary diagnosis of patients with multiple trauma in emergency situations. Rofo 166:382–388

10. Boehm T, Alkadhi H, Schertler T, Baumert B, Roos J, Marincek B, Wildermuth S (2004) Application of multislice spiral CT (MSCT) in multiple injured patients and its effect on diagnostic and therapeutic algorithms. Rofo 176:1734–1742

11. Diederich S, Lenzen H (2000) Radiation exposure associated with imaging of the chest: comparison of different radiographic and computed tomography techniques. Cancer 89:2457–2460

12. Landis JR, Koch GG (1977) The measurement of observer agreement for categorical data. Biometrics 33:159–174

13. Novelline RA, Rhea JT, Rao PM, Stuk JL (1999) Helical CT in emergency radiology. Radiology 213:321–339

14. Linsenmaier U, Krotz M, Hauser H, Rock C, Rieger J, Bohndorf K, Pfeifer KJ, Reiser M (2002) Whole-body computed tomography in polytrauma: techniques and management. Eur Radiol 12:1728–1740

15. Voggenreiter G, Aufmkolk M, Majetschak M, Assenmacher S, Waydhas C, Obertacke U, Nast-Kolb D (2000) Efficiency of chest computed tomography in critically ill patients with multiple traumas. Crit Care Med 28:1033–1039

16. Alkadhi H, Wildermuth S, Desbiolles L, Schertler T, Crook D, Marincek B, Boehm T (2004) Vascular emergencies of the thorax after blunt and iatrogenic trauma: multi-detector row CT and three-dimensional imaging. Radiographics 24:1239–1255